ELSEVIER

Journal of Structural Geology 28 (2006) 1214–1227

JOURNAL OF STRUCTURAL GEOLOGY

www.elsevier.com/locate/jsg

Structural evolution and permeability of normal fault zones in highly porous carbonate rocks

L. Micarelli [a,*], A. Benedicto [a], C.A.J. Wibberley [b]

[a] *Dpt. Science de la Terre, Groupe Dyn. Syst. Faillés, UMR 7072, Université Paris Sud XI, 91405 Orsay, France*
[b] *UMR Géoscience Azur, Université de Nice-Sophia Antipolis, 250, rue A.Einstein, 06560 Valbonne, France*

Received 6 September 2005; received in revised form 3 February 2006; accepted 22 March 2006

Abstract

The structural evolution of cataclastic fault cores from nucleation to growth was studied for the case of normal fault zones affecting high-porosity carbonates in the Hyblean Plateau, Sicily. A comparison was made between faults with increasing displacements affecting a similar lithology at shallow depth conditions. In the first few millimetres to centimetres adjacent to the fault surface, porosity is significantly reduced by a sequence of pore collapse, grain crushing, rotation-enhanced abrasion and calcite precipitation, which is a function of increasing displacement. Consequently, fault planes have strongly reduced permeability even for very small displacements. Adjacent damage zones are characterized by fracture density and connectivity increasing toward the fault plane. Cataclastic rock production and consequent fault-core development initiate as the fault displacement reaches values of 1–5 m. This displacement threshold coincides with a decrease in the widening of the damage zone per unit increase of fault displacement, which relates to a change in the mechanism of deformation accumulation in the fault zone. The change is interpreted to result from strain-softening in the fault zone due to the onset of cataclasis. Permeability data indicate that normal faults in high-porosity carbonates are effective transversal seals even at very small offsets and their combined conduit-barrier hydraulic behaviour is accentuated as displacement increases. These results show some similarities but key differences with respect to fault zone development for the analogous cases of sandstones and low-porosity limestones.

Keywords: Cataclasis; Fault core; Damage zone; Porosity; Permeability; Fault displacement

1. Introduction

Two structural components characterize well developed fault zones: a damage zone and a fault core (e.g. Chester and Logan, 1986; Chester et al., 1993; Caine et al., 1996). They may have different permeability properties due to different structural fabrics and deformation mechanisms (e.g. Antonellini and Aydin, 1994, 1995; Evans et al., 1997; Knipe, 1997; Wibberley and Shimamoto, 2003). Damage zones consist of rock volumes affected by fault-related fracturing. Bedding surfaces and inherited structural fabrics are commonly preserved (e.g. Billi et al., 2003). Fault cores, where the majority of displacement is accommodated, usually consist of cataclastic rocks. Pre-existing structures are thus obliterated during progressive cataclastic flow as displacement increases (Chester and Logan, 1986). The size of fault cores and the presence and type of cataclastic rocks control the frictional fault properties (Morrow and Byerlee, 1989; Scott et al., 1994), the hydrodynamic behaviour of faults during earthquake slip events (Wibberley, 2002; Wibberley and Shimamoto, 2005) and indeed the three-dimensional permeability patterns around faults (e.g. Caine et al., 1996).

According to Shipton and Cowie (2001), a fault zone is a four-dimensional system involving slip along the main fault surface and deformation within a volume around that surface, both of which accumulate through time. This accumulation through time is, however, difficult to characterize, even when cross-cutting relationships are available to constrain relative timing. One way to overcome this difficulty is to infer the temporal evolution of fault zone architectures by comparing faults affecting similar lithologies in the same geological context, with different displacement magnitudes, the assumption being that faults with small displacements represent the early stages of growth of larger faults. This approach may be

* Corresponding author. Now at: BEICIP-FRANLAB, 232, Av. Napoléon Bonaparte, BP 213, 92502 Rueil-Malmaison, France.
E-mail address: luca.micarelli@beicip.fr (L. Micarelli).

0191-8141/$ - see front matter © 2006 Published by Elsevier Ltd.
doi:10.1016/j.jsg.2006.03.036

used to document how the fault zone varies in width and structural complexity as a fault grows (e.g. Aydin and Johnson, 1978; Antonellini and Aydin, 1994; Knott et al., 1996; Shipton and Cowie, 2001).

An understanding of the onset of cataclastic fault-rock production and fault-core development is crucial because of their influence on fault zone permeability and frictional properties. Mechanisms that develop cataclastic rocks in fault cores may vary in space and time, and cannot be depicted by a single relationship (Blenkinsop, 1991; Storti et al., 2003; Billi and Storti, 2004). Fault-core, cataclastic rock and damage zone evolution has been investigated in sandstone and crystalline basement rocks, yet much less information is available for carbonate rocks (Hadizadeh, 1994; Billi et al., 2003; Micarelli et al., 2003; Storti et al., 2003; Billi and Storti, 2004; Micarelli et al., in press).

In this paper, we present structural data from normal fault zones in highly porous carbonate rocks from the Hyblean Plateau, southeastern Sicily. We study the evolution of the fault zone architecture and describe the structural style at the outcrop- and grain-scales, via systematic sampling and microstructural analyses. We focus on the mechanisms leading to cataclastic rock production in fault cores and investigate the onset of fault-core development as a function of displacement magnitude. By integrating these observations, with an analysis of permeability, we build a picture of damage zone and core evolution through displacement accumulation. Consequently, we discuss the implications of fault zone architectural evolution on the hydraulic behaviour of fault zones in highly porous carbonates.

2. Geological setting

The Hyblean Plateau dominates southeastern Sicily (Fig. 1a). It is part of the emerged foreland of the Neogene–Quaternary Maghrebian thrust belt and was deformed by different fault systems related to extensional and strike-slip tectonics that are still active (e.g. Torelli et al., 1998; Monaco and Tortorici, 2000). These fault systems are associated with extensive Upper Miocene–Lower Pleistocene volcanic activity and uplift. They bound and control the development of major Plio-Pleistocene basins such as the Gela–Catania foredeep, flanking the northwestern margin of the Hyblean Plateau. The thrust front runs from Catania to Gela, its frontal part being buried by sediments of Early Pleistocene age (Grasso et al., 1995). Minor basins developed on the Ionian side of the Plateau and have been related to the activity on the Malta escarpment (Grasso and Lentini, 1982; Adam et al., 2000) in a general framework of ESE–WNW regional extension (Tortorici et al., 1995; Monaco and Tortorici, 2000; Cifelli et al., 2004).

On the Hyblean Plateau, exposed sedimentary rocks are mainly of Tertiary age (Rigo and Barbieri, 1959; Grasso and Lentini, 1982) and deposited in a foreland basin setting. Geographically, the succession can be divided into eastern and western facies (Fig. 1b; Grasso et al., 1982; Lentini, 1984). The eastern succession, which is largely exposed on the Ionian margin of the Hyblean Plateau, consists of Oligocene–Miocene shallow water carbonates with intercalated volcanic rocks (Grasso et al., 1982). They rest upon carbonates of Late Cretaceous–Paleogene age and volcanic rocks, which are remnants of earlier platforms and volcanic seamount sequences (Adam et al., 2000). The western succession consists of Upper Oligocene–Miocene shelf carbonates and marls, which rest upon mainly pelagic carbonate rocks of Late Cretaceous–Eocene age. Messinian volcanic intercalations are locally present (Montenat, 1990; Lentini, 1984). Both carbonate successions are mostly composed of calcarenites, coarse carbonate breccias, bioclastic grainstones, calcarenites interbedded with marl–lime mudstones, and marls. Most lithologies have high porosity.

The structural setting of the Hyblean Plateau is governed by two main interacting coeval fault systems, oriented approximately NE–SW and NW–SE (Fig. 1b). Most faults are normal dip-slip and are related to several weak tectonic events of different ages. The NE–SW trend is sub-parallel to the faults flanking the northern Hyblean margin and to the buried front of the thrust belt that runs ENE–WSW close to the southern slope of Mt. Etna (Torelli et al., 1998). The NW–SE faults are more common in the Ionian side of the Plateau and run sub-parallel to the Malta Escarpment (Torelli et al., 1998).

We study several normal fault zones cropping out on the Hyblean Plateau. We compare faults with different amounts of displacement to infer the temporal evolution of fault zone architectures, based on the following considerations. (i) All the studied faults are related to weak tectonic events. They showed displacements ranging from zero to a few tens of metres. (ii) All the studied faults affect similar carbonate series, i.e. massive or poorly-layered, highly porous calcarenites. (iii) The Hyblean Plateau has never been strongly buried, which implies that faulting took place at very shallow depths, or at the surface. The maximum burial depth for the fault zones studied is estimated at 150–200 m, based on field stratigraphic data.

3. Methods

We investigated 27 fault zones (Table 1) by measuring structural elements and sampling zones of cataclasite, fractures and host-rock along scan lines. In the field, the fault core is distinguished from the surrounding damage zone by the occurrence of cataclastic rocks (e.g. Sibson, 1977; Billi et al., 2003). The core is commonly sharply bounded on one or both sides by major fault surfaces. Damage zones gradually fade outward into intact host-rock or protolith. Their distinction from the protolith is based on the change in the density and geometry of fault-related fractures, although the boundary is gradational.

The microstructures of the samples collected were analysed with standard transmitted light microscopy. Fifty thin sections, 30 of which were impregnated with blue epoxy, were examined to determine mineralogy and texture, to recognize the possible presence of cements and to estimate qualitatively the porosity.

Permeability was measured using the high confining pressure (200 MPa), fluid-flow apparatus at Geosciences Azur, Université de Nice–Sophia Antipolis. The pressure

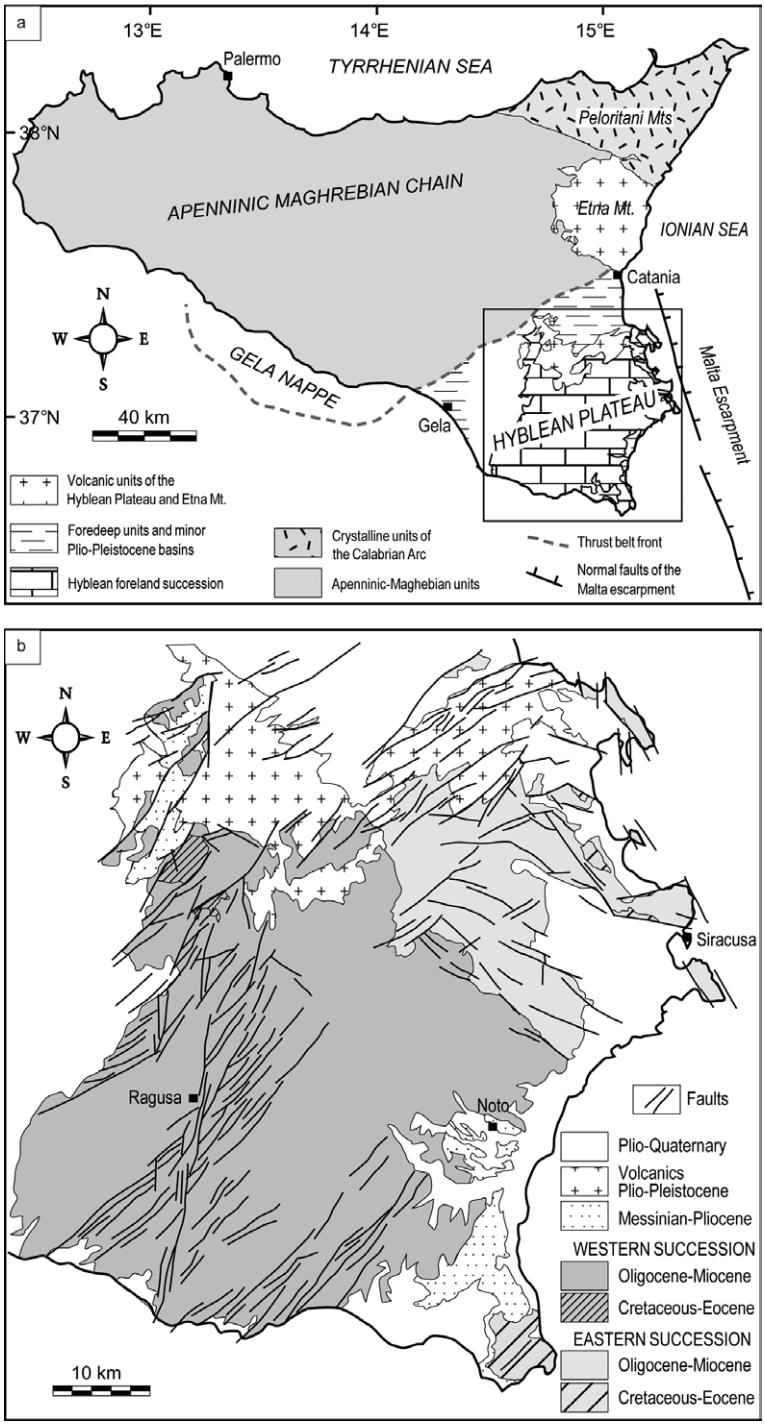

Fig. 1. (a) Map of Sicily, showing the main structural domains at the regional scale. Inset indicates the study area. (b) Simplified geological map of the Hyblean Plateau showing the main outcropping faults and the overall distribution of the Cretaceous–Miocene carbonate facies, divided into eastern and western successions.

vessel subjected samples to uniform confining pressure (Pc; isotropic stress) that could be increased. Oil was used as a confining medium and nitrogen gas as a pore fluid, at room temperature. Permeability was measured by the constant flow-rate technique with pore fluid-pressure differences of 0.1–0.5 MPa, vented to atmospheric pressure at the downstream end. The samples were subjected to an initial confining pressure of 10 MPa. The confining pressure was then increased in steps of 10 MPa up to 60 MPa. Permeability data are reported as a function of the confining pressure. Cylindrical samples were prepared in the laboratory from oriented blocks of different fault rocks collected along traverses across the fault zones. The cores used had diameters of 20 mm and lengths of between 20 and 40 mm. Each sample was placed between perforated steel spacers and further jacketed with the end pistons before being inserted into the pressure vessel.

Table 1
Summary of fault zone data. For each studied fault the displacement amount, the damage-zone width and the presence and type of fault core are noted. Porosity-reduction mechanisms are also shown and defined by a number: (1) localized compaction of the finest size fraction of the sediment, (2) fossil shell crushing, (3) rotation-enhanced particle abrasion of larger particles, and (4) precipitation of calcite cement

Fault	Displacement (m)	DZ width (cm)	Fault core	Porosity reduction mechanisms			
				1	2	3	4
F1	0.04	35	No core	X			
F2	0.1	40	No core	X			
F3	0.1	65	No core	X			
F4	0.2	100	No core	X			
F5	0.2	40	No core	X			
F6	0.25	60	No core	X			
F7	0.25	100	No core	X			
F8	0.35	55	No core	X			
F9	0.4	100	No core	X			
F10	0.7	150	No core	X	X		
F11	0.9	75	No core	X			
F12	1	250	No core	X			
F13	1.2	250	Discontinuous core	X	X		
F14	1.3	100	Discontinuous core	X	X		
F15	1.4	250	Discontinuous core	X	X		
F16	1.8	180	Discontinuous core	X	X		
F17	2	300	Discontinuous core	X	X		
F18	4	280	Discontinuous core	X	X		
F19	6	300	Continuous core		X	X	
F20	7.2	310	Continuous core		X		
F21	8	340	Continuous core		X		
F22	10	240	Continuous core		X	X	
F23	12	350	Continuous core		X		
F24	15	400	Continuous core		X	X	
F25	16	370	Continuous core		X	X	X
F26	20	480	Continuous core		X	X	X
F27	30	370	Continuous core		X	X	X

4. Fault zone analysis

The normal fault zones analysed show a large variety of structural architectures. However, in general they contain discrete, single and planar slip surfaces or localised slip zones. All of the faults studied contain damage zones, but only some have fault cores (Table 1).

4.1. Damage zones

Damage zones are characterized by the presence of fault-related fractures (Kim et al., 2004). No offset or very small offset is accumulated by minor faults in damage zones (Fig. 2), almost the entire displacement being localized in the central slip surface or slip zone of the fault. Most fault-related fractures are shear fractures or joints and strike sub-parallel to the fault strikes. However, fractures are both synthetic and antithetic to the faults and also vertical fractures occur. The different fracture dip angles produce different degrees of connectivity within the fracture networks.

Connectivity is a fundamental property of fracture populations with respect to fluid flow and can be evaluated semi-quantitatively by assessing the degree of physical connection among fractures within a network (Fig. 3a; Ortega and Marrett, 2000; Micarelli et al., 2004). The ratio of the number of fractures that are isolated (type I), simply-connected (type II), or multiply-connected (type III) divided by the total number of fractures in the network may be illustrated, using a triangular diagram (Fig. 3b). The degree of connectivity strongly increases from the protolith-damage zone boundary towards the fault plane. In particular, connectivity was defined for three domains (Fig. 3): fault core, *intensely deformed damage zone* (IDDZ), and *weakly deformed damage zone* (WDDZ). IDDZs are distinguished by densely spaced fractures, synthetic or antithetic to the fault, which are typically connected forming lozenge-shaped lithons, as opposed to the less frequent sub-vertical fractures in WDDZ (Fig. 2; Micarelli et al., 2003, in press). IDDZs define commonly sharp zones of deformation, in places bounded by minor slip surfaces; also for faults having small displacement (e.g. Fig. 4). The overall sizes of the IDDZs are approximately between a third and a fifth of the sizes of the whole damage zones.

4.2. Fault cores and cataclastic rocks

Fault cores are up to a few tens of centimetres wide, with small grain size and porosity. They are bounded on one or both sides by slip surfaces, upon which all the displacement localises. In the fault core, rock fabric changes from fracture-dominated to cataclastic. Pre-existing sedimentary or tectonic structures are obliterated due to particle rotation, attrition and translation, i.e. cataclastic flow.

Fault cores (and cataclastic rocks) only occur along faults with a displacement more than about 1 m (Fig. 5). Faults with

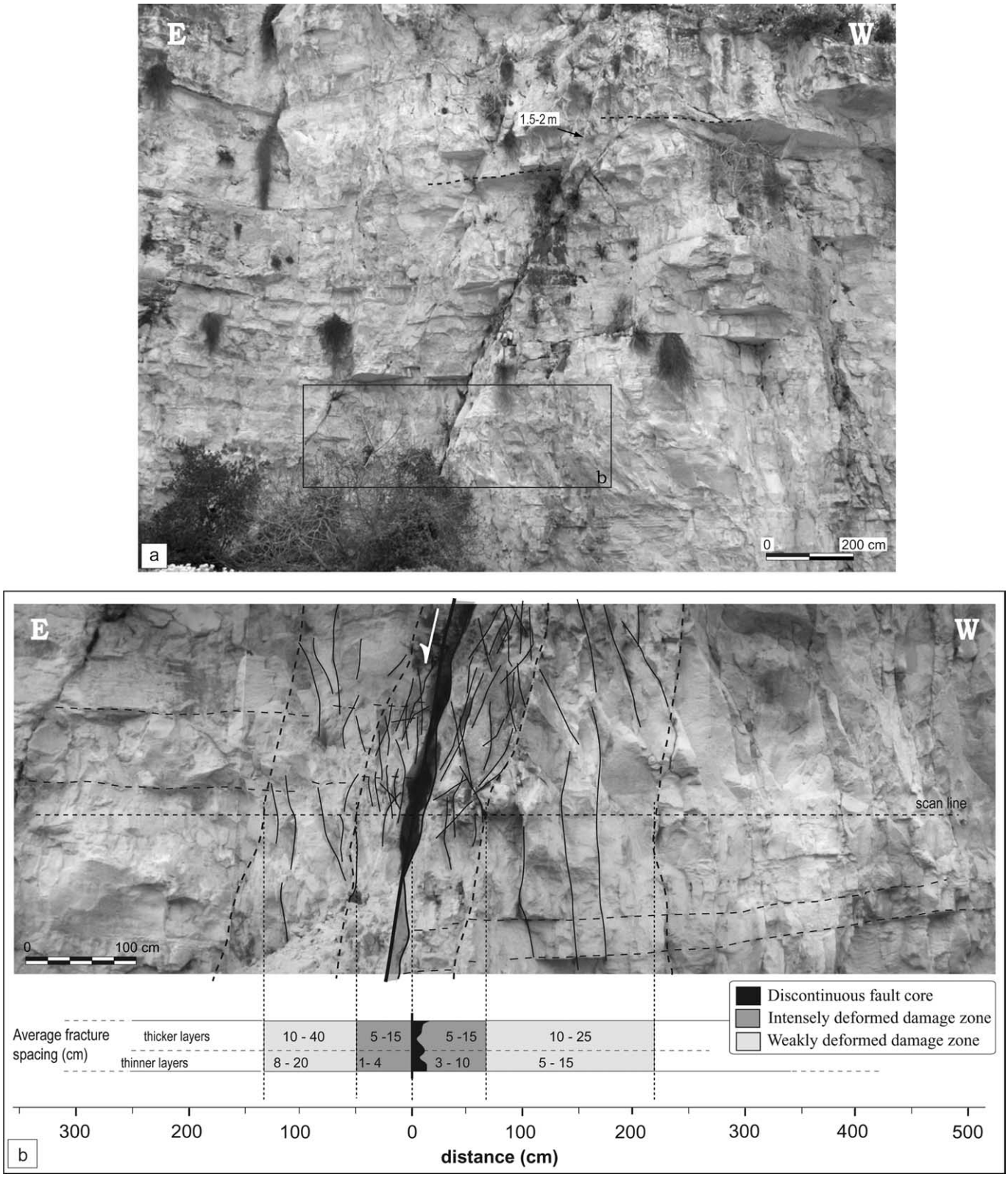

Fig. 2. Scicli survey site. (a) Fault zones are commonly characterized by a single, straight central slip surface, which accumulates the total fault offset. Here the fault has a displacement of about 1.5–2 m and displays a discontinuous fault core with protocataclasites and cataclasites. Inset indicates location of (b). (b) Scan line across the fault zone. Structural domains (weakly deformed damage zone, intensely deformed damage zone and fault core) are distinguished based on geometry and spacing of fractures and presence of cataclastic rocks.

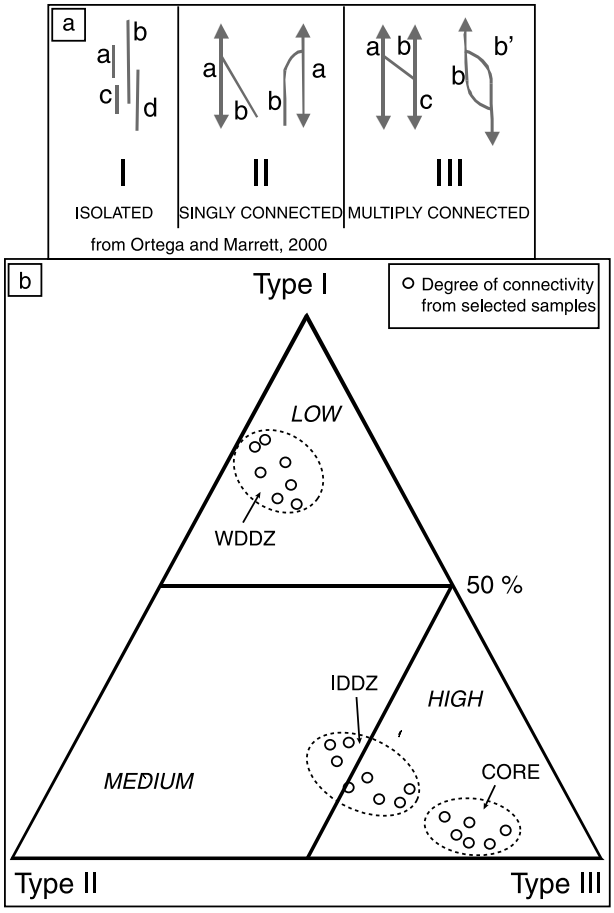

Fig. 3. (a) Sketch showing the different types of physical connection between fractures. (b) Degree of connectivity of fracture networks within the calcarenites across some studied fault zones. Connectivity increases from the damage zone to the fault core. Note in particular the low degree of connectivity in the weakly deformed damage zone (WDDZ) and the higher connectivity in the intensely deformed damage zone (IDDZ).

displacements of between around 1 and 5 m show discontinuous, narrow cores (e.g. Fig. 2). Cataclastic rocks develop where the fault plane has irregularities or bends, or where different lithologies are juxtaposed across the fault plane. Faults with displacements of more than 5 m display continuous fault cores bounded on one side by the fault surface (Fig. 6a). The core width along the fault can vary strongly, probably as a function of lithological changes.

Fault rocks occurring in fault cores are commonly poorly indurated protocataclasites and cataclasites (Fig. 6b; *sensu* Sibson, 1977). Cataclasite fragments mainly consist of single grains and fossil shells from calcarenites, grain and fossil fragments and larger (up to a few centimetres) multigrain, angular calcarenite clasts (Fig. 6c). They are surrounded by a finer calcareous cataclastic matrix, which is significantly more abundant in the first few millimetres adjacent to the slip surface. A small amount of calcite cement has been observed in only three of the nine continuous cores of the faults with the largest displacements (a few tens of metres).

Faults with continuous fault cores also have bands, up to 50 cm thick, consisting of incohesive protobreccia and highly fractured carbonates (Fig. 6). Calcarenite clast sizes are up to

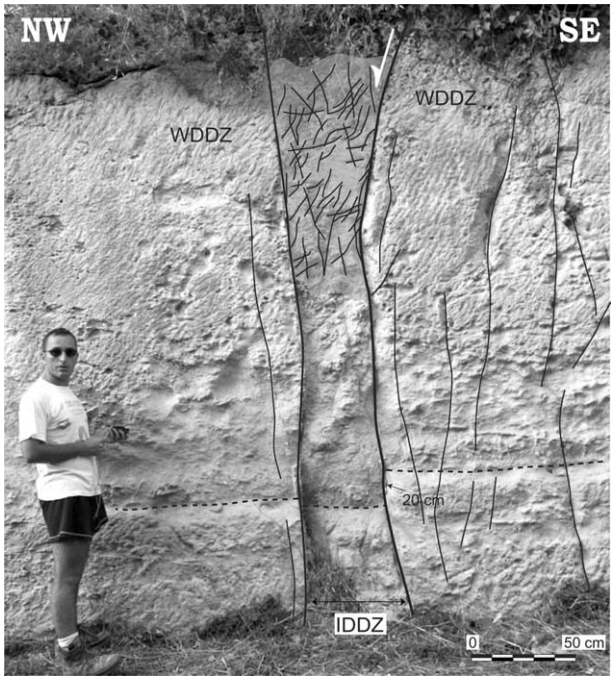

Fig. 4. Cassaro survey site. Small-offset faults lack a fault core. However, they display well-defined WDDZ and IDDZ. The WDDZ contains some spaced, isolated sub-vertical fractures, whereas the IDDZ contains smaller, more abundant, well-connected fractures.

tens of centimetres. This domain constitutes a damage zone–fault core (DZ–FC) transition and displays a rock fabric that is both fracture-dominated and cataclastic. It shows some analogies with those described in shallow-water carbonate rocks by Billi et al. (2003), who interpreted it as the relic structure of embryonic fault cores. However, our observations highlight that the DZ–FC transition occurs only with continuous fault cores. We interpret this geometry to mean that the formation of this kind of DZ–FC transition for the studied highly porous calcarenites is late, as a consequence of increasing displacement.

4.3. Porosity reduction

A reduction in porosity adjacent to the localised slip surface with respect to the host rock is observed for all fault zones

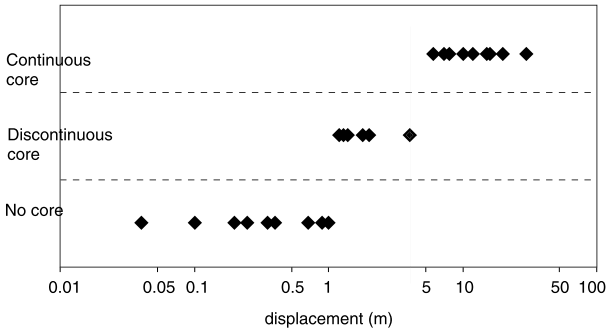

Fig. 5. Graph showing all values of fault displacement for which each of the three fault zone architectures (displaying no core, discontinuous core, or continuous core) occurs. Each point corresponds to a fault studied.

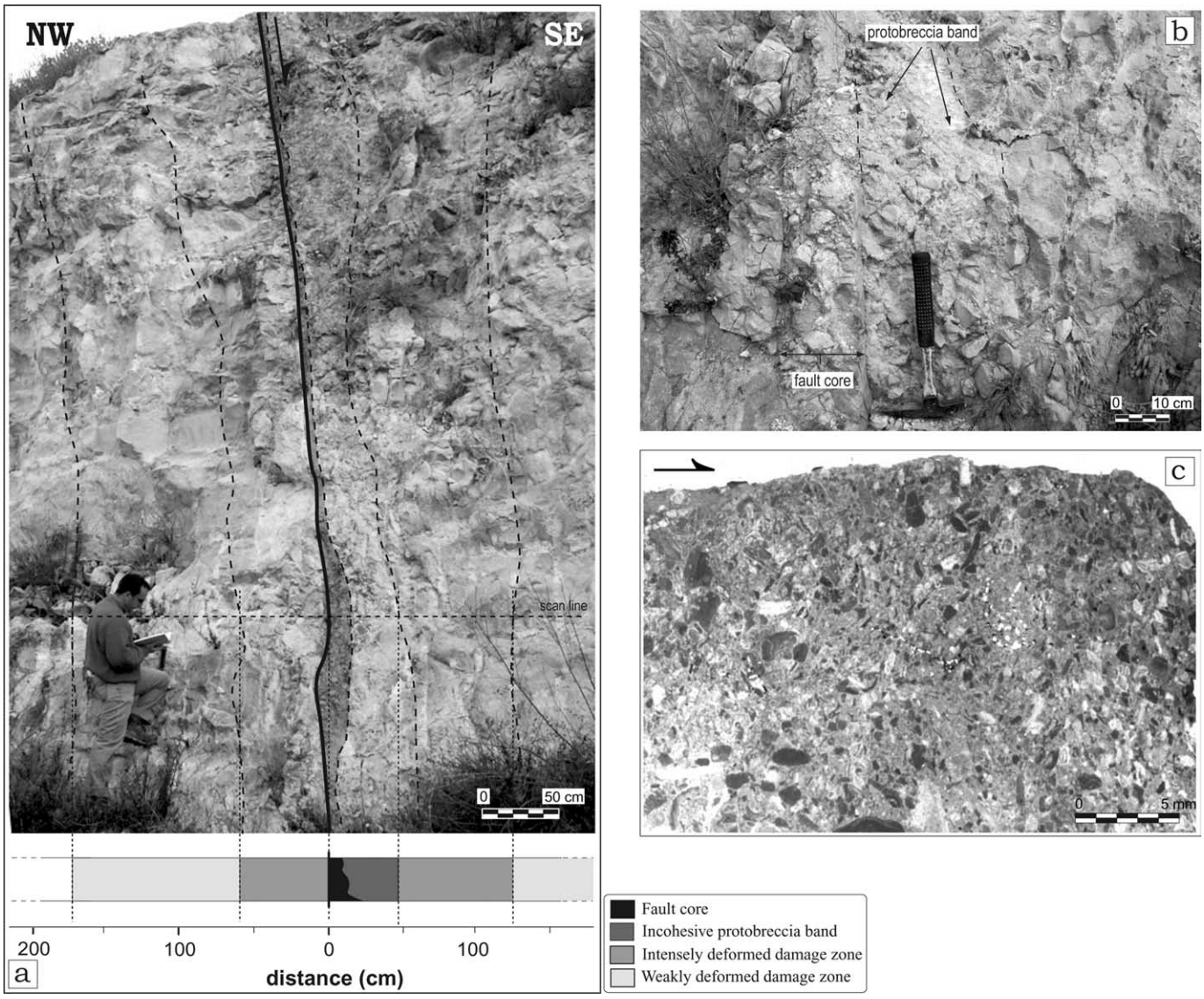

Fig. 6. Pozzallo survey site. (a) Fault with a displacement of about 10–15 m, as an example of fault zone with continuous fault core. (b) The fault core consists of indurated cataclasite, with a hanging wall transition to mainly incohesive protobreccia adjacent to the damage zone. (c) Cataclasite in the fault core consists of carbonate grain and fossil shell fragments and a finer calcareous cataclastic matrix. The black arrow shows the sense of movement on the slip surface of the fault (plain light microphotograph).

studied, irrespective of fault displacement. Yet faults with small displacements do not have cores, therefore porosity reduction is not necessarily related to fault core development, and in general characterizes only the first few millimetres (or very occasionally the first few centimetres) adjacent to the central slip surface. The host calcarenites have a high primary porosity that is related to: (i) a very high percentage of empty fossil shells; (ii) relatively large empty pores (up to approximately 1 mm wide) mainly located within the finest part of the sediment; (iii) micro-pores present in the finest part of the sediment. This last porosity is difficult to estimate, but has been recognised by increasing enlargements using standard optical microscopy.

Thin-section analyses have recognized four fault-related mechanisms responsible for decreased porosity in proximity of the fault slip surface (Table 1):

1. Pore collapse in the finest size fraction of the sediment, which leads to the disappearance of both large and micro-pores (Fig. 7a–c). It probably occurred by localized compaction and re-organisation along grain boundaries.
2. Grain (mainly empty fossil shell) crushing. The shells are commonly broken without being completely fragmented (Fig. 7a, b, f and g). Therefore, porosity is lost but shell fragments keep their shapes. With increasing particle fragmentation, shells are commonly completely crushed. Pore collapse and grain crushing can yield preferential re-orientation of elongated grains and shells (Fig. 7b).
3. Rotation-enhanced particle abrasion of larger particles during shear (Fig. 7d–g). Particle abrasion yields an increase in the relative content of fine particles (the cataclasite matrix) with respect to the content of

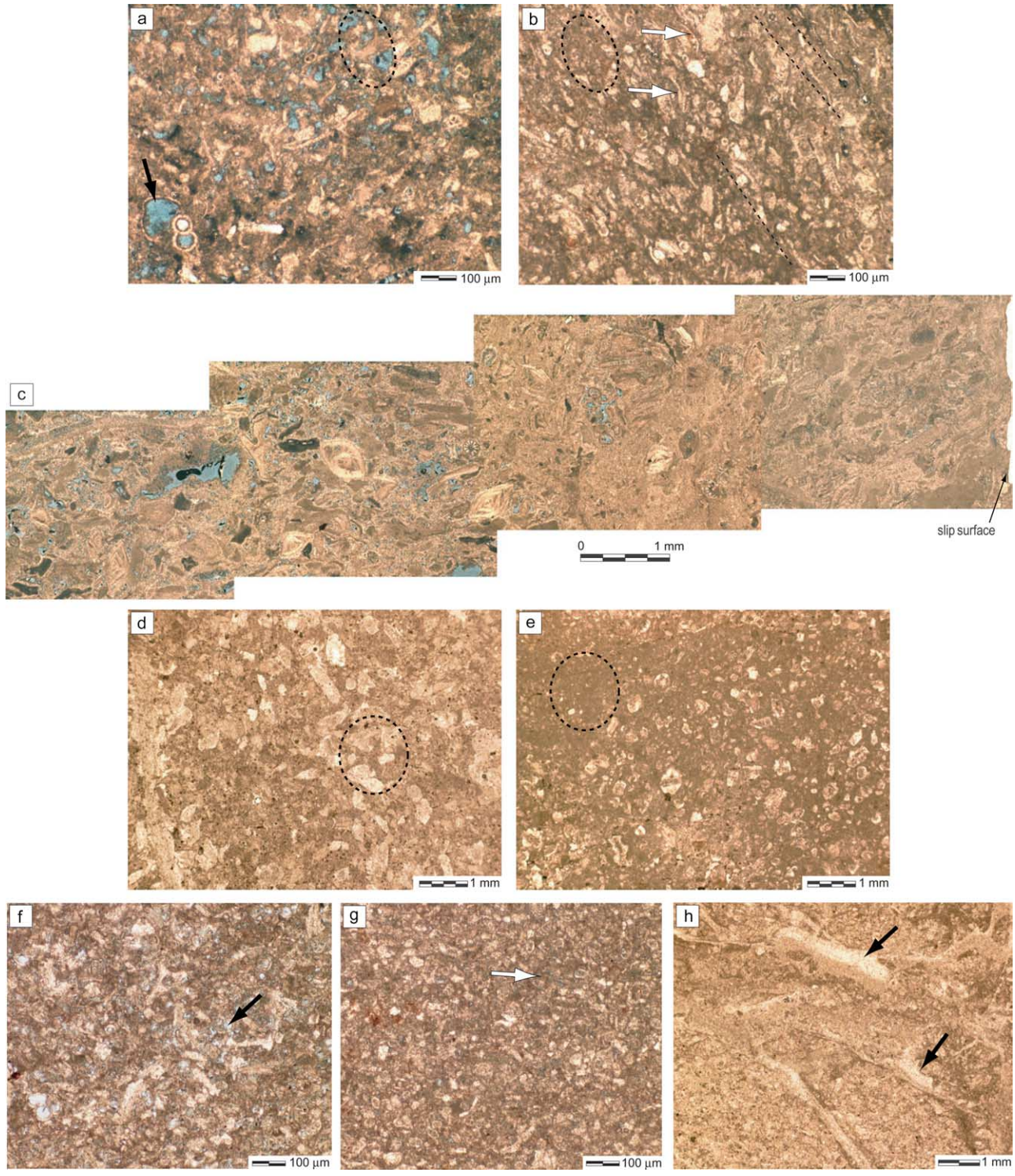

Fig. 7. Plain light microphotographs of calcarenite samples at different distances from the slip surfaces of the studied faults (blue: impregnation of the epoxy resin in pores). (a) and (b) Fault with displacement of 70 cm. Samples at (a) 1 cm away from the slip surface, and (b) on the slip surface, respectively. Note the porosity reduction due mostly to pore collapse in the finest size fraction of the sediment (e.g. compare circled zones in the two pictures), fossil shell crushing (black arrow shows intact shell; white arrows indicate broken shells) and preferential re-orientation of elongated shells (dashed lines indicate trends of preferred orientation). (c) Fault with displacement of 100–120 cm. The strong porosity reduction is due to pore collapse in the finest size fraction of the sediment. Note that porosity reduction is localized in only a few millimetres close to the slip surface, at the right edge of this photomosaic transect. (d) and (e) Fault with displacement of about 10 m. Sample (d) is from the footwall damage zone a few centimetres away from the fault plane and (e) from the fault core, respectively. Significant production of cataclastic matrix (compare circled zones in the two pictures) suggests that porosity reduction is due mostly to abrasion of the larger particles. (f), (g) and (h) Fault with displacement of 20 m. (f) Sample from the protolith consisting of highly porous fine calcarenites. (g) Sample a few centimetres away from the fault plane. Porosity is reduced by fossil shell crushing (note intact shells arrowed) and particle abrasion (cataclastic matrix is arrowed). (h) Sample from the fault core. Calcite cement (black arrows) fills relatively late fractures and relict porosity.

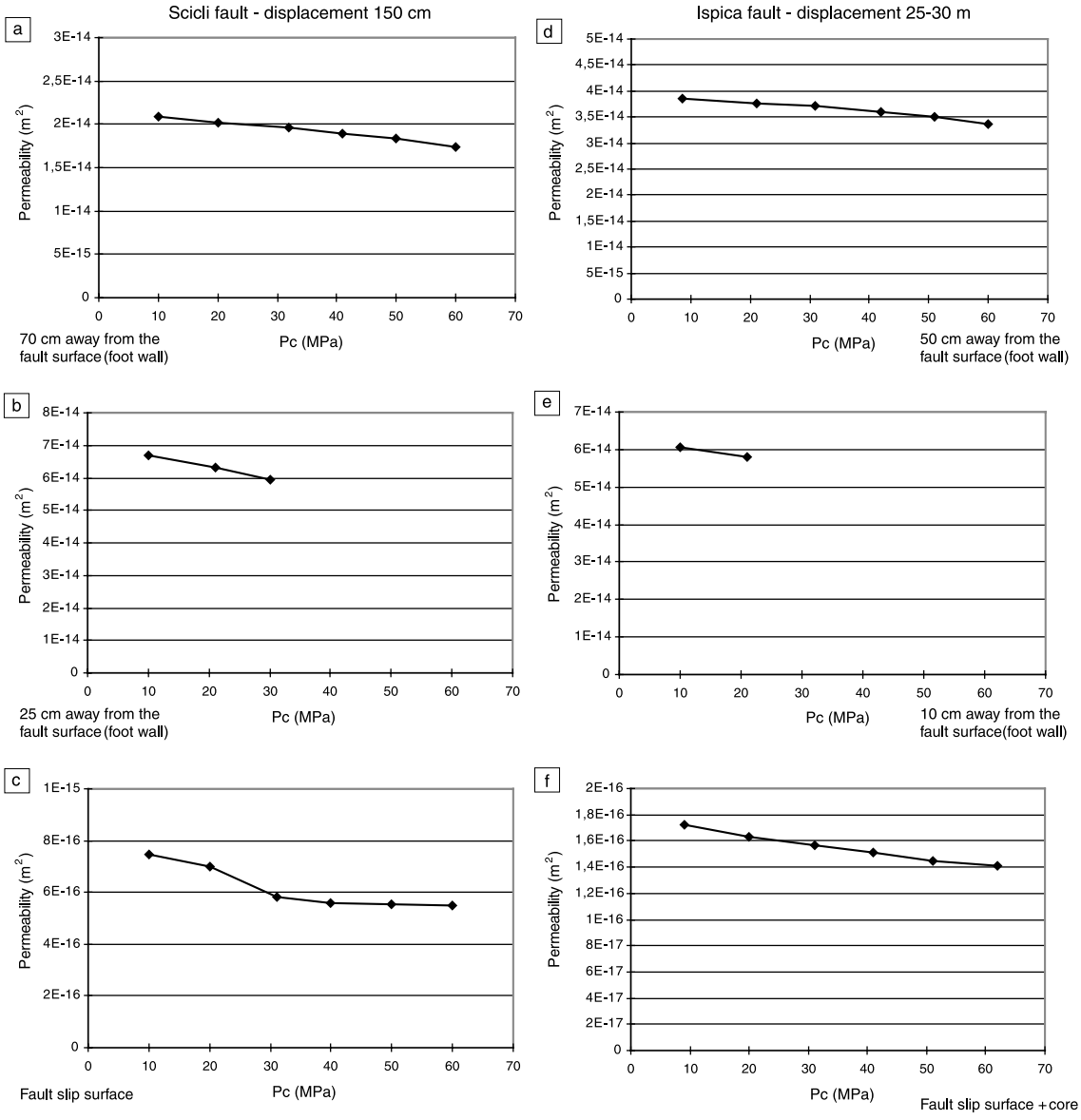

Fig. 8. Permeability data: selected samples at difference distances from the central slip surface of faults. (a)–(c) The samples are from a fault zone with a displacement of 1.5 m and discontinuous fault core. (d)–(f) Samples from a fault zone with a displacement of 25–30 m and continuous fault core. Pc denotes confining pressure.

coarse particles (Hooke and Iverson, 1995; Billi and Storti, 2004; Billi, 2005).

4. Precipitation of calcite cement in newly-formed fractures and eventually in relict porosity (Fig. 7h). Calcite cement consists of subhedral crystals (up to 100 μm in width), which suggests probable growth in free-fluid conditions (e.g. Canole et al., 1997; Micarelli et al., 2005). Cement precipitation is observed only in a few fault cores and has a subordinate and late role in sealing fault-core porosity.

In some fault cores these four porosity-reduction mechanisms coexist. More typically, they are sequential as a function of displacement magnitude and thus one (or more) mechanism(s) commonly predominated at a particular stage of fault evolution (Table 1).

4.4. Permeability data

Permeability measurements were conducted on a few samples to test if porosity reduction correlates to decreasing permeability. Samples from faults affecting massive or poorly layered, high-porosity calcarenites, were measured to compare results for a single lithology.

Permeability measurement samples fall into two classes of permeability data:

1. Samples collected from the protolith and from damage zones between 100 and 20 cm away from the fault planes show permeabilities in the order of 10^{-14} m^2 at a confining pressure (Pc) varying between 10 and 60 MPa (Fig. 8a, b, d and e).
2. Samples comprising the central slip surface of the faults, and the core if present, have lower permeabilities, of about

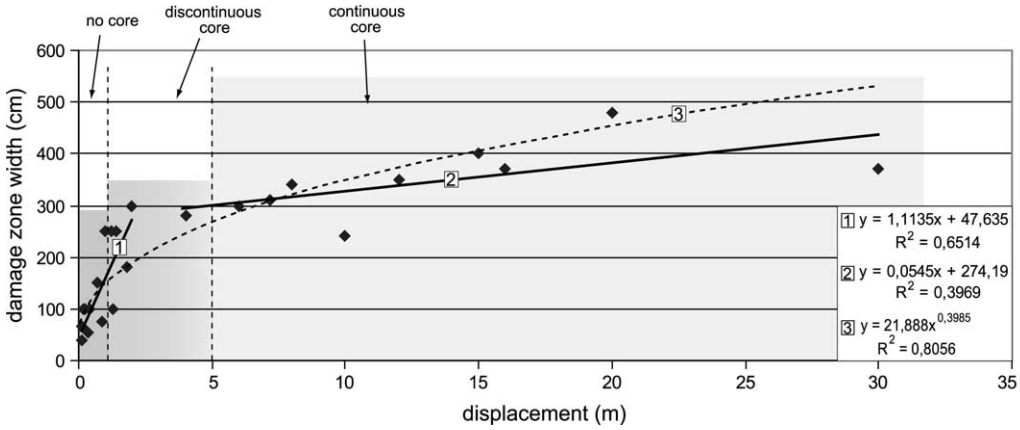

Fig. 9. Graph of damage zone widths vs. fault displacements. Data are fitted by either one power-law relationship (dashed line 3) or two distinct straight lines with different slopes (solid lines 1 and 2). Fields corresponding to faults (i) with no cataclastic core, (ii) with discontinuous core, and (iii) with continuous core are also shown.

10^{-16} m^2 at a Pc varying between 10 and 60 MPa (Fig. 8c and g). Measurements were made on core samples oriented perpendicular to the fault.

The data show that the samples comprising the fault slip surface, and in places the fault core, have a permeability about two orders of magnitude lower than the adjacent damage zones and host-rocks. The data show a low sensitivity of permeability to confining pressure for all samples (Fig. 8), which suggests a relatively low compressibility of pores to be crushed. Furthermore, permeability values and their variations with distance from the fault surface are independent of fault displacement magnitude, as shown for the samples from faults with displacements of 1.5 m and 25–30 m (Fig. 8). It must be noted that the fault-core sample of the Ispica fault ($d \sim 25$–30 m; Fig. 8f) has a permeability $\sim$3–4 times less than the slip surface sample of the Scicli fault ($d \sim 1.5$ m; Fig. 8c). Although this difference may signify a decrease in permeability as comminution proceeds with increasing displacement to produce a continuous fault core, the slip surface in the Scicli fault sample is narrower than the sample length, so the measured permeability may reflect the higher permeability of the surrounding rock. In other words, the sample is heterogeneous on the scale of the structures of interest, causing a possible scale problem. Nevertheless, the decrease in permeability for both faults appears to be concentrated in the first few millimetres adjacent to the central slip surface, which correlates with the zone where porosity reduction is observed.

4.5. Correlations between damage zone width and fault displacement

Changes in the density and geometry of fault-related fractures provide a means for defining the edges of damage zones and evaluating the sizes of the fault zone components as a function of displacement. A plot of damage zone widths, summed for hanging wall and footwall, versus fault displacements shows that the damage zone width is in general larger for faults having greater offsets (Fig. 9). This correlation implies that deformation is accommodated within the damage zone as offset is accumulated after a through-going slip surface has developed (e.g. Fossen and Hesthammer, 2000; Shipton and Cowie, 2001, 2003).

The data are best fitted by either one power-law relationship or two distinct straight lines with different slopes (dashed and solid lines, respectively, in Fig. 9). Either way, the slope of the relationship is greater for faults with small displacements. The slope becomes less in a relatively sharp transition zone located between fault displacement values of 1.5 and 5 m. Assuming that faults with small displacements represent the early stages of development of larger faults, the amount of the damage-zone width increase per unit of fault displacement is greater during the early stages of fault evolution and sharply decreases over some displacement threshold, which corresponds to the curve break.

5. Discussion

5.1. Fault architecture evolution

Based on field data, textural relationships and permeability tests, we subdivided the evolution of near-surface fault zone in high-porosity carbonates into three stages (Fig. 10).

5.1.1. Faults with displacements lower than 1 m

Faults with displacements smaller than 1 m lack fault cores and cataclastic rocks (Fig. 10a). The fault is a well-defined, approximately planar surface, which accommodates all offset. The fault zone structure is characterized by a damage zone in which fracture density and connectivity increase towards the fault plane. The IDDZ commonly varies in width, has sharp boundaries and is characterized by highly connected fractures. Porosity reduction is located in the first few millimetres adjacent to the fault surface, with the collapse of large and micro-pores in the finest size fraction of the sediment, due mostly to localized compaction (mechanism 1, see Section 4.3),

The small-displacement faults described here seem not to develop from any evident pre-existing structures, such as veins

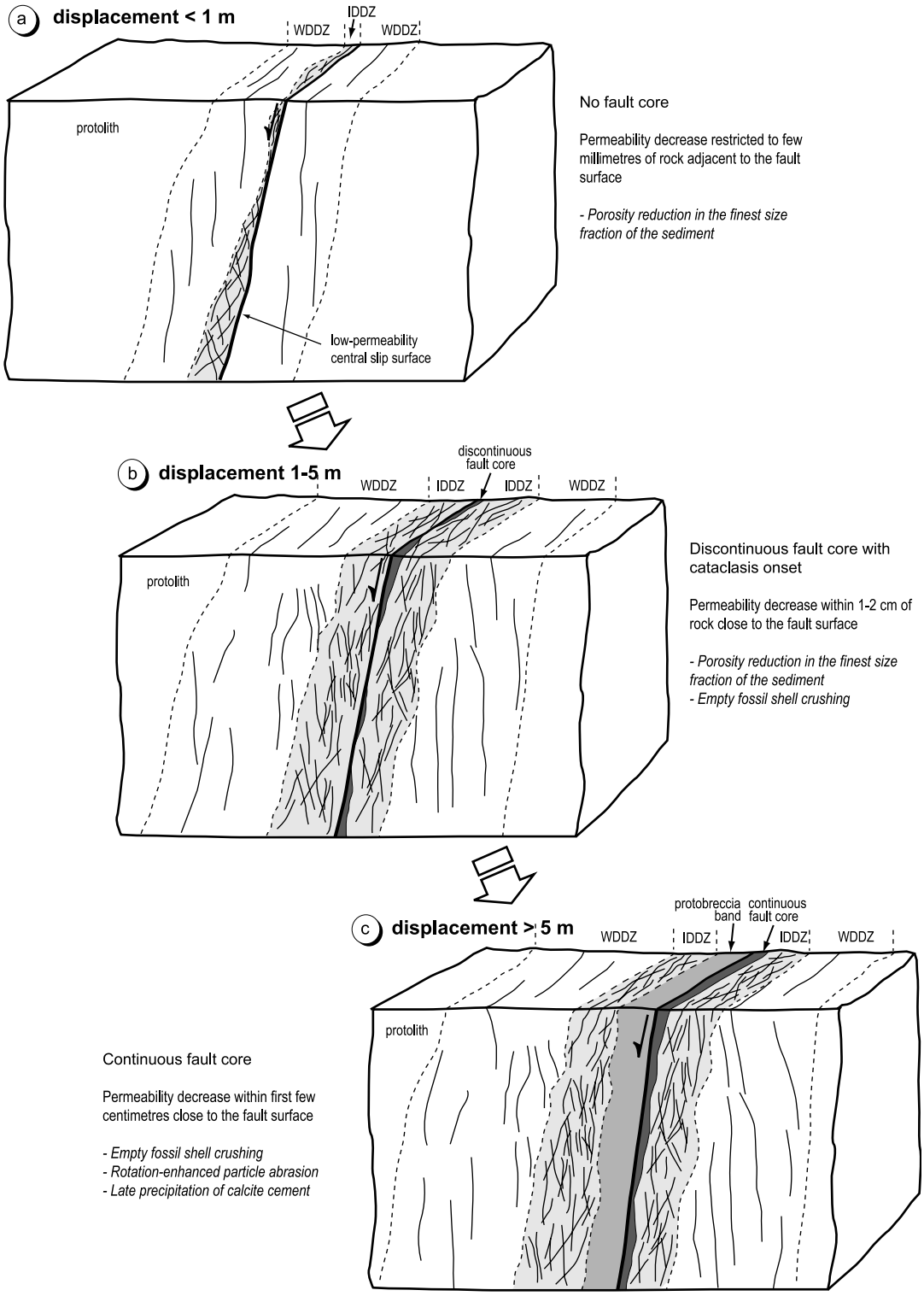

Fig. 10. Sketch showing a conceptual model for fault architecture evolution in the studied highly porous carbonate rocks. (a) Faults with displacements smaller than 1 m do not show a fault core. The WDDZ and the IDDZ are characterized by different fracture density and connectivity. (b) Faults with displacements from 1 to 5 m show discontinuous fault cores related to cataclasis. Damage zone widths strongly increase with displacement. (c) Faults with displacements larger than 5 m show continuous fault cores and commonly a protobreccia band. Damage zone widths show little increase with displacement. During the three stages faults have low-permeability slip surfaces, but the mechanisms of porosity reduction change with increasing displacement.

or solution seams. According to the existing literature, this is very unlikely to happen (see e.g. Crider and Peacock, 2004 for a review). Although an examination of the nucleation of the fault slip surfaces is not the aim of this paper, some observations on the role played by possible precursor structures are pertinent (Crider and Peacock, 2004). The small-displacement faults studied do not show the same characteristics as deformation bands in high-porosity sandstone, such as the lack of

a well-defined discontinuity plane and typical connecting eye and ramp structures among different segments (e.g. Antonellini et al., 1994; Antonellini and Aydin, 1995). However, the porosity reduction and, in places, the preferential re-orientation of elongated grains associated with very small displacements without significant grain fracturing, suggest that deformation bands with no cataclasis could act as precursor structures (e.g. Antonellini et al., 1994; Swierczewska and Tokarski, 1998). It is worth noting that the well-defined, planar slip surfaces described here from high-porosity calcarenites are absent in the first stages of deformation band generation in high-porosity sandstone (e.g. Aydin and Johnson, 1983; Shipton and Cowie, 2001). This interesting contrast is probably due to the properties of the carbonate lithology affected, the calcarenites studied being quite indurated and competent, although cement is not present. This characteristic is likely to enhance strain softening and the development of a slip surface (Rudnicki and Rice, 1975; Mair et al., 2000), rather than strain hardening and localization of other deformation bands in proximity of the first one, as commonly described in porous sandstones (Rudnicki and Rice, 1975; Aydin and Johnson, 1983).

5.1.2. Faults with displacements from 1 to 5 m

As displacement increases, faults develop a discontinuous fault core, constituted by narrow bands of breccia and cataclasite (Fig. 10b). The IDDZs widen and display highly connected shear fractures. The main mechanisms of porosity reduction are pore collapse in the finest size fraction of the sediment and particle fragmentation, mostly crushing of the empty fossil shells (mechanisms 1 and 2, see Section 4.3). Porosity reduction is localized in the first tens of millimetres adjacent to the central slip surface and correlates to a strong permeability decrease.

5.1.3. Faults with displacements larger than 5 m

A well-developed, narrow and continuous fault core characterizes faults with the largest displacements (Fig. 10c). The core contains poorly indurated cataclasites, with locally abundant matrix. A damage zone–fault core (DZ–FC) transition, consisting of mainly incohesive protobreccia and highly fractured carbonates, is commonly present. The IDDZ width remains mostly unchanged and again is defined by intense, highly connected fractures. Porosity reduction characterizing fault cores is related to crushing of the empty fossil shells, rotation-enhanced particle abrasion of larger particles (becoming more important as fault offset increases; see also Billi, 2005) and late, subordinate precipitation of calcite cement (mechanisms 2, 3 and 4, see Section 4.3). The permeability decrease is about the same order of magnitude as for faults with smaller throws and without cement precipitation.

5.2. Onset of cataclastic rock production and damage zone width

In the fault zones studied, the onset of cataclastic rock production occurs for displacement amounts varying between approximately 1 and 2 m. Cataclastic behaviour correlates with the first appearance of a discontinuous fault core, which becomes continuous as fault displacement exceeds about 5 m. A graph relating damage zone widths to fault offsets has a flatter curve over a threshold falling between displacement values of about 1–1.5 and 5 m, corresponding to the displacement interval in which cataclastic fault rock production begins.

The onset of cataclastic processes constitutes a threshold over which the mechanism of deformation accumulation changes, given the combination of cataclasis and significant decrease in rate of widening of the damage zone per unit increase in displacement. After a continuous fault core has developed by cataclastic processes, the greater part of strain is accommodated within it, although little deformation is still being accommodated within the damage zone. The development of a continuous fault core appears therefore to act as a strain softening mechanism, which leads to deformation localization. This role of the fault core is enhanced by the lack or scarcity of calcite cement that is usually an efficient healing process in fault zones within carbonates (e.g. Micarelli et al., 2005 and references therein). If the fault zone remains weak then deformation may preferentially take place along the fault surface rather than in the surrounding rock (Segall and Pollard, 1983). Other factors that might control damage zone width, such as lithological variability and fault linkage, are not considered here because the studied faults affect similar massive lithologies, have relatively small throws and lack displacement anomalies and change in fault strike, which are characteristic of faults that developed by segment linkage (Peacock and Sanderson, 1991; Dawers and Anders, 1995).

5.3. Influence on fluid flow properties

The changing fault zone architecture, with the absence or presence of a fault core, and the localised porosity and permeability reduction have important consequences for the time and space evolution of the overall fault permeability structure. Faults with small offsets do not display a fault core, but porosity and permeability reduction occurs mostly by compaction localized in the first few millimetres adjacent to the fault surface, which can therefore constitute a narrow but relatively efficient barrier to fluid flow. Therefore, porosity destruction and permeability reduction begin relatively early in the fault evolution. These faults show a hydraulic behaviour similar to that of deformation bands in clastic rocks, which can be effective lateral seals for hydrocarbon and water even at very small offsets (e.g. Antonellini and Aydin, 1994, 1995; Shipton et al., 2002). On the other hand, IDDZs are characterized by high fracture connectivity even for small throws and can act as self-enhancing conduits for along-fault fluid flow. This permeability behaviour, particularly for the initial stage of fault evolution, is different from that presented for faults affecting limestones with relatively low porosity (Billi et al., 2003). These faults have a conduit stage, which precedes the development of the fault core, during which the progression of fracturing increases the permeability of the fault

zone. Thus, the original grain size and porosity in carbonates can significantly influence the permeability of faults, particularly for small displacements and during formation in near-surface conditions.

After the onset of cataclasis, a fault core develops, first discontinuous and then continuous along the fault zone. Cores show strong porosity and permeability reduction, due mostly to cataclastic mechanisms, such as particle fragmentation and rotation-enhanced particle abrasion. Continuous cores act as efficient barriers to transverse fluid flow. Highly connected shear fractures characterize the IDDZs and in contrast may facilitate along-fault fluid flow. In this stage, the contrast between high-permeability damage zones and low-permeability fault cores accentuates the combined conduit-barrier behaviour of fault zones with respect to fluid flow.

Calcite precipitation was evidenced in only a few, relatively large-throw faults and only as a late-stage process. The few fractures filled by calcite cement cut the low-porosity fault cores and are probably related to repetitive slip events within the core. No calcite has been found outside the fault cores. The scarcity and the late timing of cement precipitation suggest that it is a consequence rather than a cause of permeability reduction. In highly porous, nearly massive calcarenites, nothing prevents fluids from flowing out and escaping quickly, which avoids any early mineral precipitation. However, faults with large throws, highly fractured IDDZs and well-sealed continuous fault cores may contemporaneously harness along-fault flow and act as barriers to transverse fluid flow, thus enhancing the potential for calcite mineralization. This state contrasts to fault-zone development in low-porosity, well-layered limestones where calcite precipitation has been often recognized as a major and early process in faulting initiation and sealing (e.g. Crider and Peacock, 2004; Micarelli et al., 2005 and references therein).

6. Conclusions

Integrating macro- and micro-analyses, we have studied near-surface normal fault zones affecting high-porosity calcarenites of the Hyblean Plateau, Sicily. We provide a model for the evolution of the fault zones by comparing faults that have different amounts of displacement.

Faults with displacements of less than 1 m lack a fault core. Faults with displacements ranging from 1 to 5 m have discontinuous cores, whereas large-offset faults show continuous cores, consisting of cataclastic rocks. Damage-zone width-increase per unit of fault displacement is higher in an early stage of fault evolution and sharply decreases when displacement magnitude reaches 1.5–5 m. This fault displacement threshold corresponds to the onset of cataclasis and consequent fault-core development. After the fault core nucleates, it accommodates most of the further strain and the damage zone then accommodates relatively little further deformation. This has important implications for studying relationships between damage-zone width and displacement for normal faults in highly porous carbonates, because damage zones can remain narrow even if the fault accumulates a large displacement.

In all the faults studied, porosity is significantly reduced in the first few millimetres adjacent to the central slip surface by: (i) localized compaction of the finest size fraction of the sediment, (ii) fossil shell crushing, (iii) rotation-enhanced particle abrasion of larger particles, and (iv) precipitation of calcite cement as a function of increasing displacement. Porosity reduction relates to a permeability decrease of two orders of magnitude with respect to that of the host-rock, for both small- and large-offset faults. Therefore, the early sealing of small-offset faults, lacking a core, is not related to either cement precipitation or cataclastic rock production.

The fault slip surfaces are relative barriers for fluids even at very small offsets, whereas highly-fractured damage zones may enhance fluid flow. This combined conduit-barrier hydraulic behaviour is accentuated in large-offset fault zones due to: (i) progression of fracturing and fracture connectivity in the intensely deformed damage zone, and (ii) fault core sealing by increasing cataclastic processes and possible cement precipitation.

Acknowledgements

This work has been carried out in the framework of a research agreement between TOTAL and the University of Paris XI (DGEP/TDO/CA/RD n. 12806A1/UPS n. 6052 1/CNRS: 041.1883.01). We thank Sylvie Delisle and Jean-Loup Montenat (TOTAL) for the facilities and helpful discussions. We thank the TOTAL-Pau laboratories and Jean-Pierre Villotte (Université Paris XI) for the preparation of samples and thin sections. We also thank Yves Missenard for the help and suggestions on the fieldwork and interpretations and Olivier Gerbaud for the helpful discussions. The very constructive reviews of Atilla Aydin and William M. Dunne significantly improved the manuscript.

References

Adam, J., Reuther, C.D., Grasso, M., Torelli, L., 2000. Active fault kinematics and crustal stresses along the Ionian margin of the southeastern Sicily. Tectonophysics 326, 217–239.

Antonellini, M., Aydin, A., 1994. Effect of faulting on fluid flow in porous sandstones: petrophysical properties. American Association of Petroleum Geologist Bulletin 78, 355–377.

Antonellini, M., Aydin, A., 1995. Effect of faulting on fluid flow in porous sandstones: geometry and spatial distribution. American Association of Petroleum Geologist Bulletin 79, 642–671.

Antonellini, M., Aydin, A., Pollard, D.D., 1994. Microstructure of deformation bands in porous sandstones at Arches National Park, Utah. Journal of Structural Geology 16, 941–959.

Aydin, A., Johnson, A.M., 1978. Development of faults as zones of deformation bands and as slip surfaces in sandstones. Pure and Applied Geophysics 116, 931–942.

Aydin, A., Johnson, A.M., 1983. Analysis of faulting in porous sandstones. Journal of Structural Geology 5, 19–31.

Billi, A., 2005. Grain size distribution and thickness of breccia and gouge zones from thin (<1 m) strike-slip fault core in limestone. Journal of Structural Geology 27, 1823–1837.

Billi, A., Storti, F., 2004. Fractal distribution of particle size in carbonate cataclastic rocks from the core of a regional strike-slip fault zone. Tectonophysics 384, 115–128.

Billi, A., Salvini, F., Storti, F., 2003. The damage zone-fault core transition in carbonate rocks: implication for fault growth, structure and permeability. Journal of Structural Geology 25, 1779–1794.

Blenkinsop, T.G., 1991. Cataclasis and processes of particle size reduction. Pure and Applied Geophysics 136, 59–86.

Caine, J.S., Evans, J.P., Forster, C.B., 1996. Fault zone architecture and permeability structure. Geology 24, 1025–1028.

Canole, P., Odonne, F., Polve, M., 1997. Heterogeneous strain associated with normal faulting: evidence of mass transfer by pressure solution associated with fault displacement. Tectonophysics 283, 129–143.

Chester, F.M., Logan, J.M., 1986. Composite planar fabric of gouge from the Punchbowl Fault, California. Journal of Structural Geology 9, 621–634.

Chester, F.M., Evans, J.P., Biegel, R.L., 1993. Internal structure and weakening mechanisms of the San Andreas fault. Journal of Geophysical Research 98, 771–786.

Cifelli, F., Rossetti, F., Mattei, M., Hirt, A.M., Funiciello, R., Tortorici, L., 2004. An AMS structural and paleomagnetic study of quaternary deformation in eastern Sicily. Journal of Structural Geology 26, 29–46.

Crider, J.G., Peacock, D.C.P., 2004. Initiation of brittle faults in the upper crust: a review of field observations. Journal of Structural Geology 26, 691–707.

Dawers, N.H., Anders, M.A., 1995. Displacement-length scaling and fault linkage. Journal of Structural Geology 17, 607–614.

Evans, J.P., Forster, C.B., Goddard, J.V., 1997. Permeabilities of fault-related rocks and implications for fault-zone hydraulic structure. Journal of Structural Geology 19, 1393–1404.

Fossen, H., Hesthammer, J., 2000. Possible absence of small faults in the Gullfaks Field, northern North Sea: implication for downscaling of faults in some porous sandstones. Journal of Structural Geology 22, 851–863.

Grasso, M., Lentini, F., 1982. Sedimentary and tectonic evolution of the eastern Hyblean Plateau (southeast Sicily) during Late Cretaceous to Quaternary times. Palaeogeography Palaeoclimatology Palaeoecology 39, 261–280.

Grasso, M., Lentini, F., Pedley, H.M., 1982. Late Tortonian–Lower Messinian (Miocene) palaeogeography of SE Sicily: information from two new formations of the Sortino Group. Sedimentary Geology 32, 279–300.

Grasso, M., Miuccio, G., Maniscalco, R., Garofalo, P., La Manna, F., Stamilla, R., 1995. Plio-Pleistocene structural evolution of the western margin of the Hyblean Plateau and the Maghrebian foredeep, SE Sicily. Implications for the deformational history of the Gela Nappe. Annales Tectonicae 9, 7–21.

Hadizadeh, J., 1994. Interaction of cataclasis and pressure solution in a low-temperature carbonate shear zone. Pure and Applied Geophysics 143, 255–280.

Hooke, R.LeB., Iverson, N.R., 1995. Grain-size distribution in deforming subglacial tills: role of grain fracture. Geology 23, 57–60.

Kim, Y-S., Peacock, D.C.P., Sanderson, D.J., 2004. Fault damage zones. Journal of Structural Geology 26, 503–517.

Knipe, R.J., 1997. Juxtaposition and seal diagrams to help analyze fault seals in hydrocarbon reservoirs. American Association of Petroleum Geologists Bulletin 81, 187–195.

Knott, S.D., Beach, A., Brockbank, P.J., Brown, J.L., Mc Callum, J.E., Welbon, A.I., 1996. Spatial and mechanical controls on normal fault populations. Journal of Structural Geology 18, 359–372.

Lentini, F., 1984. Carta Geologica della Sicilia sud-orientale. Università di Catania. S.E.L.C.A. (Eds.), scale 1:100000.

Mair, K., Main, I., Elphick, S., 2000. Sequential growth of deformation bands in the laboratory. Journal of Structural Geology 22, 25–42.

Micarelli, L., Moretti, I., Daniel, J.M., 2003. Structural properties of rift-related normal faults: the case study of the Gulf of Corinth, Greece. Journal of Geodynamics 36, 275–303.

Micarelli L., Daniel J.M., Moretti I., 2004. Structural characteristics of Quaternary fault zones in the south-western Gulf of Corinth (Greece). Proceeding of the workshop COST-ACTION 625. Studi Geologici Camerti, Special Issue/2004.

Micarelli, L., Benedicto, A., Invernizzi, C., Saint-Bezar, B., Michelot, J.L., Vergely, P., 2005. Influence of P/T conditions on the style of normal fault initiation and growth in limestones from the SE-Basin, France. Journal of Structural Geology 27, 1577–1598.

Micarelli, L., Moretti, I., Jaubert, M., Moulouel, H., in press. Fracture analysis in the south-western Corinth rift (Greece) and implications for fault hydraulic behaviour. Tectonophysics.

Monaco, C., Tortorici, L., 2000. Active faulting in the Calabrian arc and Eastern Sicily. Journal of Geodynamics 29, 407–424.

Montenat, J.L., 1990. Evolution structurale du Plateau Ibléen (Sicile, Italie) dans le cadre de l'arc Tyrrehenien. Unpublished Ph.D. Thesis, University of Nancy.

Morrow, C.A., Byerlee, J.D., 1989. Experimental studies of compaction and dilatancy during frictional sliding on faults containing gouge. Journal of Structural Geology 11, 815–825.

Ortega, O., Marrett, R., 2000. Prediction of macrofracture properties using microfracture information, Mesaverde Group sandstones, San Juan basin, New Mexico. Journal of Structural Geology 22, 571–588.

Peacock, D.C.P., Sanderson, D.J., 1991. Displacement, segment linkage and relay ramps in normal fault zones. Journal of Structural Geology 13, 721–733.

Rigo, M., Barbieri, R., 1959. Stratigrafia pratica applicata in Sicilia. Bolletino del Servizio Geologico Italiano 80, 1–92.

Rudnicki, J.W., Rice, J.R., 1975. Conditions for the localization of deformation in pressure-sensitive dilatant materials. Journal of the Mechanics and Physics of Solids 23, 371–394.

Scott, D.R., Marone, C.J., Sammis, C.G., 1994. The apparent friction of granular fault gouge in sheared layers. Journal of Geophysical Research 99, 7231–7246.

Segall, P., Pollard, D.D., 1983. Nucleation and growth of strike-slip faults in granite. Journal of Geophysical Research 88, 555–568.

Shipton, Z.K., Cowie, P.A., 2001. Damage zone and slip-surface evolution over μm to km scales in high-porosity Navajo sandstone, Utah. Journal of Structural Geology 23, 1825–1844.

Shipton, Z.K., Cowie, P.A., 2003. A conceptual model for the origin of fault damage zone structures in high-porosity sandstone. Journal of Structural Geology 25, 333–344.

Shipton, Z.K., Evans, J.P., Robeson, K.R., Forster, C.B., Snelgrove, S., 2002. Structural heterogeneity and permeability in faulted eolian sandstone: implications for subsurface modelling of faults. American Association of Petroleum Geologist Bulletin 86, 863–883.

Sibson, R.H., 1977. Fault rocks and fault mechanisms. Journal of the Geological Society 133, 191–231.

Storti, F., Billi, A., Salvini, F., 2003. Particle size distributions in natural carbonate fault rocks: insights for non-self similar cataclasis. Earth and Planetary Science Letters 206, 173–186.

Swierczewska, A., Tokarski, A.K., 1998. Deformation bands and the history of folding in the Magura nappe, Western Outer Carpathians (Poland). Tectonophysics 297, 73–90.

Torelli, L., Grasso, M., Mazzoldi, G., Peis, D., 1998. Plio-Quaternary tectonic evolution and structure of the Catania foredeep, the northern Hyblean Plateau and the Ionian shelf (SE Sicily). Tectonophysics 298, 209–221.

Tortorici, L., Monaco, C., Tansi, C., Cocina, O., 1995. Recent and active tectonics in the Calabrian Arc (Southern Italy). Tectonophysics 243, 37–55.

Wibberley, C.A.J., 2002. Hydraulic diffusivity of fault gouge zones and implications for thermal pressurization during seismic slip. Earth Planets Space 54, 1153–1171.

Wibberley, C.A.J., Shimamoto, T., 2003. Internal structure and permeability of major strike-slip fault zones: the Median Tectonic Line in Mie Prefecture, Southwest Japan. Journal of Structural Geology 25, 59–78.

Wibberley, C.A.J., Shimamoto, T., 2005. Earthquake slip weakening and asperities explained by thermal pressurization. Nature 436, 689–692.